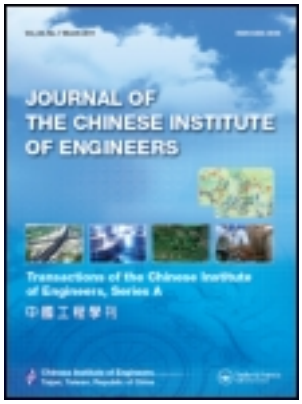

Journal of the Chinese Institute of Engineers
Publication details, including instructions for authors and subscription information:
http://www.tandfonline.com/loi/tcie20

Experimental study on seismic performance of steel beam to SRC column connections

Cheng-Chiang Weng [a] , Yen-Liang Yin [b c] , Huei-Shun Wang [d] & Chong-Han Yang [d]

[a] Department of Civil Engineering , National Chiao Tung University , 1001 Ta-Hsueh Rd., Hsinchu 300, Taiwan Phone: 886-3-5726507 Fax: 886-3-5726507 E-mail:

[b] Department of Civil Engineering , National Taiwan University , No. 1, Roosevelt Rd., Sec. 4, Taipei 106, Taiwan

[c] CEO and Chief R&D Officer, Ruentex Group , 14F, No. 308, Sec. 2, Bade Road, Taipei 104, Taiwan.

[d] Department of Civil Engineering , National Chiao Tung University , 1001 Ta-Hsueh Rd., Hsinchu 300, Taiwan

Published online: 04 Mar 2011.

To cite this article: Cheng-Chiang Weng , Yen-Liang Yin , Huei-Shun Wang & Chong-Han Yang (2008) Experimental study on seismic performance of steel beam to SRC column connections, Journal of the Chinese Institute of Engineers, 31:2, 239-252, DOI: 10.1080/02533839.2008.9671377

To link to this article: http://dx.doi.org/10.1080/02533839.2008.9671377

EXPERIMENTAL STUDY ON SEISMIC PERFORMANCE OF STEEL BEAM TO SRC COLUMN CONNECTIONS

Cheng-Chiang Weng*, Yen-Liang Yin, Huei-Shun Wang and Chong-Han Yang

ABSTRACT

The seismic performance of steel beam to steel reinforced concrete (SRC) column connections was investigated experimentally through cyclic loading tests of two full-scale specimens. In this study, the SRC column was made of a steel box section encased in reinforced concrete. The reason for using an SRC column is to take advantage of its fire resistance, structural stiffness and strength. The experimental results showed that both of the test specimens demonstrated excellent seismic resistance capability. The steel beams of the connections were able to develop plastic rotations in excess of 5.3% radians. Satisfactory interstory drift angle up to 6.2% radians was observed from the tests. The experiments also indicated that the reinforced concrete in the beam-to-column connection zone provided an "effective constraint" to the embedded portion of the steel beam in the joint. It was observed that this constraint successfully assisted the steel beam to develop a plastic hinge outside of the SRC column face. Consequently, the groove-welded joint of the steel beam to the steel box section in the SRC column was protected by the reinforced concrete and avoided possible premature failure.

Key Words: steel beam, SRC column, beam-to-column connection, full-scale specimen, cyclic loading test, plastic hinge, shear stud, seismic performance.

I. INTRODUCTION

With the fast advances in construction technologies, the concrete-steel composite structural system produces a building with advantages which include both the stiffness of reinforced concrete and the strength of structural steel. An additional merit of the concrete-encased composite structural members is that the concrete also protects the steel section from fire damage and local buckling failure.

In this study, steel beams and steel reinforced concrete (SRC) columns were chosen to create a new type of beam-to-column connection. The steel beam was selected because of the convenience in construction. The reason for using the SRC column is to take advantage of its fire resistance, structural stiffness and strength.

The SRC structural system has been successfully used in Japan for more than half a century (Wakabayashi, 1987). The Architectural Institute of Japan published its first SRC design specification in 1958 and released the latest edition in 2001 (AIJ, 2001). In the United States, the guidelines for the design of composite moment frames were introduced in the NEHRP recommended seismic provisions (FEMA, 1994). Latest design provisions of composite structures are provided in the ACI-318 code (2005), the AISC design specification (2005), and the AISC seismic provisions (2005). In Europe, the design guidelines of composite steel and concrete structures can be found in the Eurocode (1994).

In Taiwan, new buildings constructed with SRC structures have gradually increased since the Ji-Ji

*Corresponding author. (Tel/Fax: 886-3-5726507; Email: frankweng@mail.nctu.edu.tw)

C. C. Weng is with Department of Civil Engineering, National Chiao Tung University, 1001 Ta-Hsueh Rd., Hsinchu 300, Taiwan.

Y. L. Yin is with the Department of Civil Engineering, National Taiwan University, No. 1, Roosevelt Rd., Sec. 4, Taipei 106, Taiwan; CEO and Chief R&D Officer, Ruentex Group, 14F, No. 308, Sec. 2, Bade Road, Taipei 104, Taiwan.

H. S. Wang and C. H. Yang are with the Department of Civil Engineering, National Chiao Tung University, 1001 Ta-Hsueh Rd., Hsinchu 300, Taiwan.

earthquake in 1999. The Richter 7.3 magnitude earthquake caused a death toll of 2,300 people and destroyed more than 5,000 buildings. Statistics showed that the majority of the collapsed buildings were constructed with reinforced concrete. The disaster resulted in a slow down in the housing market partly because people were not confident buying reinforced concrete buildings. As a contrast, the SRC building provides a new choice for local people. According to the data released by the housing department of Taiwan in 2003, about 20% of the newly finished buildings were SRC structures. The ministry of interior affairs of Taiwan also published the first edition of the SRC building code in 2004 (MIF, 2004).

A literature survey indicated that past studies on the seismic performance of steel beam- to-SRC column connection are very limited. It was found that a majority of past research was concentrated on the steel beam to concrete filled tubular column (CFT) connections. Research results were reported by Ricles *et al*. (1996, 2004), Nishiyama *et al*. (2004), Chiew *et al*. (2001), Schneider (1997), Elremaily *et al*. (1997), Alostaz and Schneider (1996) and Azizinamini and Prakash (2004). Considering steel beam-to-SRC column connections, Chou and Uang (2002) conducted two full-scale experiments on this type of moment connection. In their study, a wide flange steel section was encased in reinforced concrete to form an SRC column. In addition, the reduced beam section (RBS) was introduced to reduce the shear demand on the connection. Both specimens were found to be able to develop plastic rotations in excess of 0.035 radians.

The objective of this research is to investigate the seismic performance of steel beam- to-SRC column connections through cyclic loading tests. It is noted that the steel beam used in this study was directly welded to the steel box in the SRC column. There was no reduction made to the flanges of the steel beam (i.e., the beam was not a "reduced beam section, RBS"), nor was a stiffened end plate or flange plate added to the connection.

II. EXPERIMENTAL PROGRAM

1. Test Setup

In this study, two full-scale steel beam-to-SRC column connections were tested. Fig. 1 shows the analogy of a test specimen simulating an exterior beam-to-column connection of a building structure subjected to lateral load. Fig. 2 illustrates the setup of the specimen on the strong floor against a reaction wall. A 1000kN MTS dynamic actuator was used to apply cyclic loading to the tip of the steel beam of the specimen. The lateral load was applied through

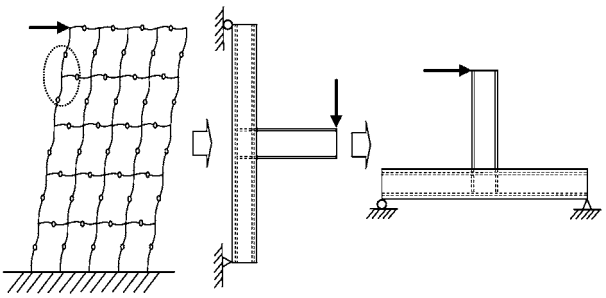

Fig. 1 Test specimen simulating an exterior steel beam-to-SRC column connection subjected to lateral load

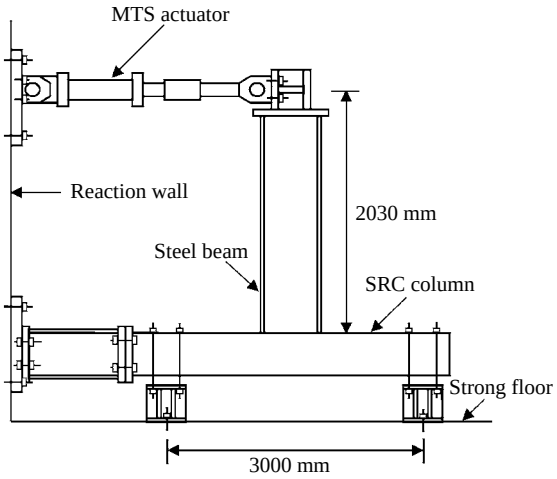

Fig. 2 Test setup of the steel Beam-to-SRC column connection in the lab

the displacement-controlled method at cyclic loading history of $0.25\Delta_y$, $0.5\Delta_y$, $0.75\Delta_y$, $1\Delta_y$, $2\Delta_y$, $3\Delta_y$ and so on until the failure of the specimen, in which Δ_y is the corresponding beam tip displacement when the steel beam starts yielding at the SRC column face. The beam tip displacement was measured by recording the horizontal travel distance of the MTS actuator at the beam tip when the strain gage reading on the steel beam flange at the SRC column face reached the yielding strain ε_y of the steel beam. To measure the rotation of the SRC column, two LVDTs were placed under the beam-to-column connection zone. The distribution of strains within the joint was traced by means of electric strain gauges that were attached to the reinforcing bars and to the steel web and flanges in the specimens.

2. Test Specimens

Figures 3(a) and (b) show the cross-sectional dimensions of the SRC columns. Each column contained a welded built-up steel box section of □ 350 × 350 × 22 × 22 mm encased by reinforced concrete.

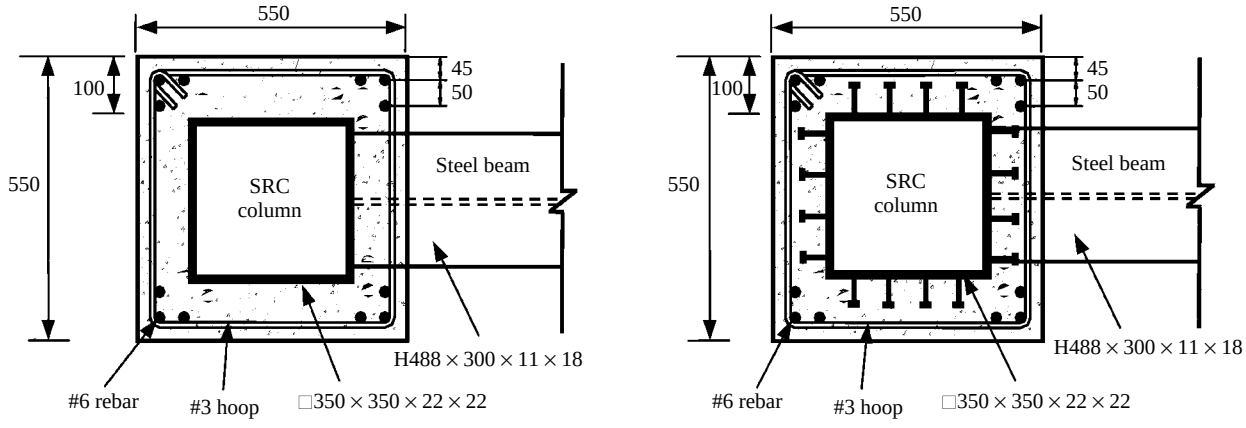

(a) Specimens SRC1–BOX–N

(b) Specimens SRC2–BOX–S

Fig. 3 Cross-sectional dimensions of the test specimens

Three #6(D19) longitudinal bars were placed at each corner of the column. A steel beam of H488 × 300 × 11 × 18 mm was grooved-welded to the steel box in the SRC column. The details of the welded joint are shown in Fig. 4. There was no reduction made to the steel beam flanges, nor was a stiffened end plate or flange plate added to the connection.

Based on a series of pilot experimental studies conducted by the authors in the structural laboratory of National Chiao Tung University (Yang, 2003; Hsu, 2003), it was found that for a steel beam connected to an SRC column, due to the "effective constraint" provided by the reinforced concrete at the connection zone of the SRC column, the steel beam was able to develop a satisfactory plastic hinge with its width-thickness ratio (b/t) designed in accordance with the "compact section" criteria in Section B4 of the AISC-LRFD specification.

These two specimens are designated as SRC1-BOX-N and SRC2-BOX-S, where the N and S indicate that the SRC column is with or without shear studs welded on the surface of the steel box. The purpose of applying shear studs in the connection zone is to investigate the influence of the studs on the ductility of the moment connection. Fig. 5 shows details of the arrangement of shear studs in the specimen SRC2-BOX-S.

As illustrated in Fig. 6, the #3(D10) hoop reinforcements were equally spaced at 150mm throughout the SRC column. Due to the existence of the steel beam in the connection zone, four L-shaped deformed bars were used to form a hoop. As shown in Fig. 4, at the bam-to- column joint, access holes for the hoop reinforcements were prepared on the steel beam web.

Photos 1 and 2 show the specimens SRC1-BOX-N and SRC2-BOX-S in preparation. Photo 3 gives a closer look of the arrangement of shear studs and hoop

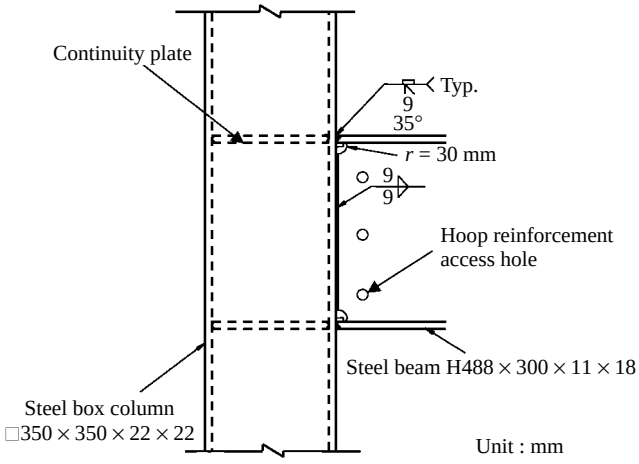

Fig. 4 Details of steel beam to steel box column welded joint

reinforcements in the connection zone of specimen SRC2-BOX-S. In Photo 4, the specimen SRC1-BOX-N is ready for the cyclic loading test. It is noted from the photo that a lateral steel brace was added to the middle height of the steel beam to avoid out-of-plane displacement during the test.

Tables 1 and 2 give the dimensions and material properties of the test specimens. The length of the SRC column is 3 m with overall cross-sectional dimension of 550 × 550 mm. The length of the steel beam is 2.03 m. The steel beam and the steel box were made of A572 Gr.50 structural steel. The yield strengths of the steel and the reinforcement are shown in the table. The average 28-day compressive strength of the concrete is 35 MPa.

In this study, both specimens were designed to meet the strong-column weak-beam requirements. Table 3 shows the ratios of moment strength at the joint of each specimen. For the strength ratio between

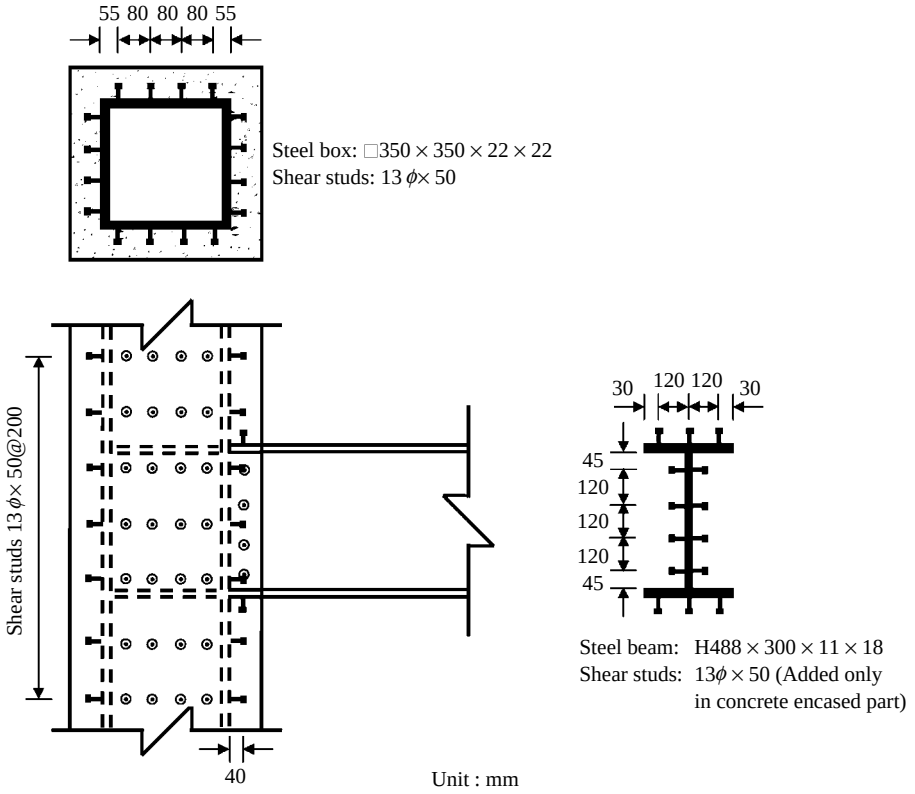

Fig. 5 Shear studs in specimen SRC2–BOX–S

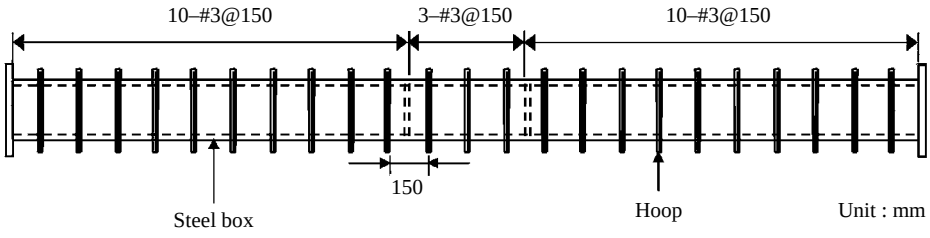

(a) Hoop reinforcements along SRC column

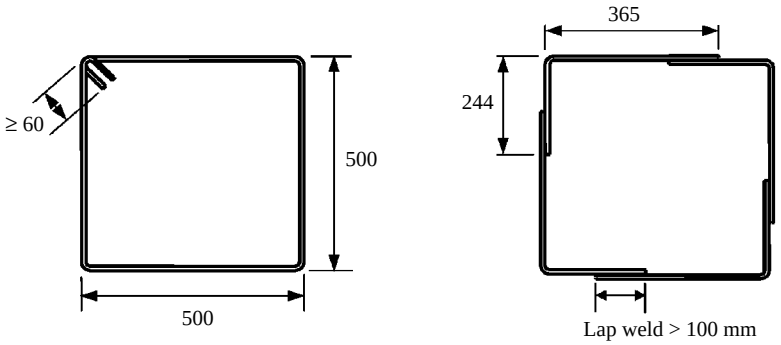

(b) Hoop in SRC column

(c) Hoop in beam-to-column joint (with 4 L-shaped #3 rebars)

Fig. 6 Arrangement of hoop reinforcements in SRC column

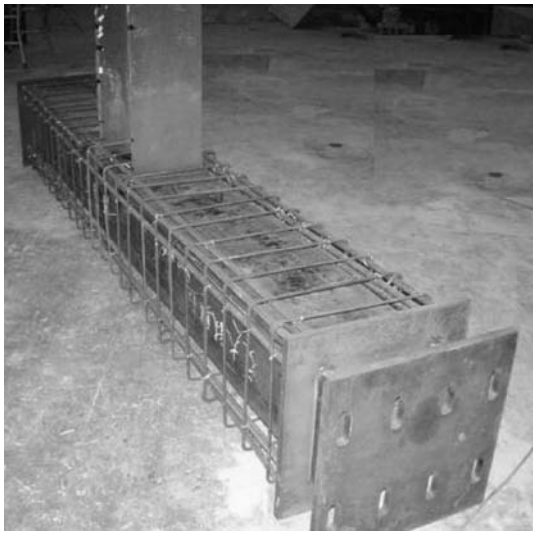

Photo 1 Specimen SRC1–BOX–N in preparation

Photo 2 Specimen SRC2–BOX–S in preparation

Photo 3 Shear studs and reinforcements at the joint of specimen SRC2–BOX–S

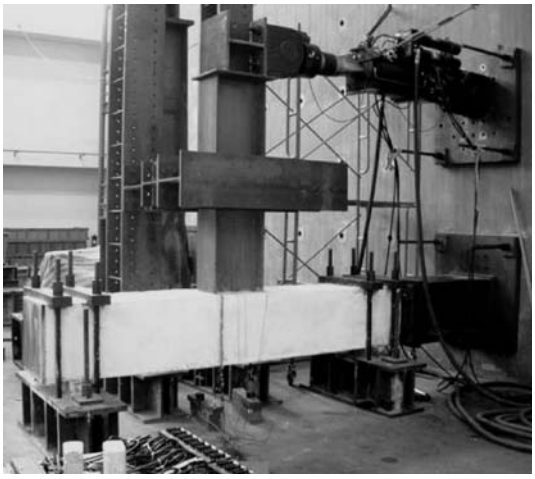

Photo 4 A steel beam-to-SRC column joint specimen ready for cyclic loading test

the steel box column and the steel beam, $\Sigma(M_{ns})_c/(M_{ns})_b$, the ratios are 2.23 and 2.26 for specimens SRC1 and SRC2, respectively. For the strength ratio between the entire SRC column and the steel beam, $\Sigma(M_{nSRC})_c/(M_{ns})_b$, the ratios are 2.84 and 2.86 for specimens SRC1 and SRC2, respectively.

In addition, Table 4 shows the ratios of the shear strength at the beam-to-column joint of each specimen. For the ratio between the nominal shear strength of the steel box section and the maximum required shear strength at the joint, $(V_n)_s/(V_u)_j$, the calculated values are 1.69 and 1.78 for specimens SRC1 and SRC2, respectively. The formulas used to calculate $(V_n)_s$ and $(V_u)_j$ are provided in the table. It is observed that, for both specimens, the nominal shear strength of the steel box section, $(V_n)_s$, is significantly larger than the maximum required shear strength of the joint, $(V_u)_j$, which occurs when the steel beam reaches its plastic moment capacity. This observation indicates that with the shear strength of the "two webs" of steel box section alone, it is strong enough to resist the maximum required shear force at the beam-to-column joint.

III. TEST RESULTS AND DISCUSSION

1. Load-Displacement Relation

Figures 7 and 8 show the load-displacement relations (hysteretic loops) of the specimens tested in this study. It is observed that both specimens demonstrated excellent ability in absorbing strain energy during the cyclic loading history. For the hysteretic

Table 1 Dimensions of the test specimens

Specimen designation	Steel beam[1]	SRC column[2]		
	Steel section $d \times b_f \times t_w \times t_f$ (mm)	Overall section $B \times D$ (mm)	Steel box section $d \times b_f \times t_w \times t_f$ (mm)	Steel ratio A_s/A_g[3] (%)
SRC1–BOX–N SRC2–BOX–S	488 ×300 ×11 ×18	550 ×550	350 ×350 ×22 ×22	9.5

Note: (1) The length of steel beam is 2030 mm. The steel beam flanges were directly groove-welded to the steel box in the SRC column. There was no reduction of the flanges of the steel beam (i.e., it was not a "reduced beam section"), nor was a stiffened-rib or flange-plate added to the steel beam at the connection zone.
(2) The length of the SRC column is 3000 mm; the spacing of the hoop reinforcement is 150 mm.
(3) A_s = area of steel box section; A_g = area of overall SRC column section.

Table 2 Material properties of the test specimens

Specimen designation	Structural steel				Reinforcement				Concrete
	Column		Beam		#3 Rebar		#6 Rebar		
	F_y (MPa)	F_u (MPa)	F_y (MPa)	F_u (MPa)	F_y (MPa)	F_u (MPa)	F_y (MPa)	F_u (MPa)	f'_c (MPa)
SRC1–BOX–N SRC2–BOX–S	403 409	529 533	415 417	535 541	427	584	502	716	35.1

Table 3 Moment strength ratio at joint: (1) Steel box column vs. Steel beam; (2) SRC column vs. Steel beam

Specimen designation	Moment strength			Moment strength ratio			
	Steel box column	SRC column	Steel beam	Steel box column to steel beam		SRC column to steel beam	
	$(M_{ns})_c$ (kN-m)	$(M_{nSRC})_c$ (kN-m)	$(M_{ns})_b$ (kN-m)	$\frac{(M_{ns})_c}{(M_{ns})_b}$	$\frac{\sum(M_{ns})_c}{(M_{ns})_b}$	$\frac{(M_{nSRC})_c}{(M_{ns})_b}$	$\frac{\sum(M_{nSRC})_c}{(M_{ns})_b}$
SRC1–BOX–N	1433	1829	1287	1.11	2.23	1.42	2.84
SRC2–BOX–S	1455	1851	1293	1.13	2.26	1.43	2.86

Note: (1) $(M_{ns})_b$ is the nominal flexural strength of the steel beam; $(M_{ns})_b = Z_b(F_{ys})_b$
(2) $(M_{ns})_c$ is the nominal flexural strength of the steel box column; $(M_{ns})_c = Z_c(F_{ys})_c$
(3) $(M_{nSRC})_c$ is the nominal flexural strength of the SRC column; $(M_{nSRC})_c = (M_{ns})_c + (M_{nrc})_c$; where $(M_{nrc})_c$ is the nominal flexural strength of the RC portion in the SRC column.

loop of specimen SRC1-BOX-N shown in Fig. 7, the positive and the negative maximum loads were +741 kN and –782 kN, respectively, when the beam tip displacement reached $7\Delta_y$. After reaching the peak load, the specimen was able to remain stable without abrupt loss of strength and stiffness. When the displacement reached $10\Delta_y$, significant plastic deformation appeared at the steel beam near the column face. The test was stopped as beam tip displacement reached $12\Delta_y$ when the load dropped to about 60% of the peak load. The final test results indicated that the connection was capable of sustaining an interstory drift angle up to 6.2% radians.

Photos 5(a) and (b) show the steel beam plastic rotations of specimen SRC1-BOX-N during the test when the angles reached 3.2% and 5.4% radians, respectively. It is observed that the steel beam developed a satisfactory plastic hinge.

Similarly, for the hysteretic loop of specimen SRC2-BOX-S shown in Fig. 8, the positive and the negative maximum loads were +739 kN and –607 kN, respectively, when the beam tip displacement reached $7\Delta_y$. The hysteretic loop also demonstrated excellent ability in absorbing strain energy. This connection was capable of sustaining an interstory drift angle of 6.7% radians. Photos 6(a) and (b) show specimen

Table 4 Shear strength ratio at joint: (1) Steel box strength vs. Required strength of joint; (2) Nominal strength of joint vs. Required strength of joint

Specimen designation	Shear strength				Shear Strength ratio	
	Nominal shear strength of Joint			Required shear strength of joint	Steel box strength of joint to maximum required strength of joint	Nominal strength of joint to maximum required strength of joint
	Steel box strength	RC portion strength	Total nominal strength			
	$(V_n)_s$[(1)] (kN)	$(V_n)_{rc}$[(2)] (kN)	$(V_n)_{j,\ SRC}$[(3)] (kN)	$(V_u)_j$[(4)] (kN)	$(V_n)_s/(V_u)_j$[(5)]	$(V_n)_{j,\ SRC}/(V_u)_j$
SRC1–BOX–N	3976	1066	5042	2351	1.69	2.15
SRC2–BOX–S	4035	1066	5101	2262	1.78	2.26

Note: (1) $(V_n)_s$ is the nominal shear strength of the steel box section.

(2) $(V_n)_{rc}$ is the nominal shear strength of the RC portion at the joint $(V_n)_{rc} = 1.0\sqrt{f_c'}\,A_j$; A_j is the shear area of the joint; f_c' : MPa

(3) $(V_n)_{j,\ SRC}$ is the nominal shear strength of the SRC joint; $(V_n)_{j,\ SRC}$ = (1) + (2)

(4) $(V_u)_j$ is the maximum required shear strength at the joint; $(V_u)_j = \dfrac{M_{pb}}{d_b - t_{bf}} - V_{col}$; M_{pb} is the plastic moment strength of the steel beam; d_b is depth of the steel beam; t_{bf} is the flange thickness of the steel beam; V_{col} is the column shear force.

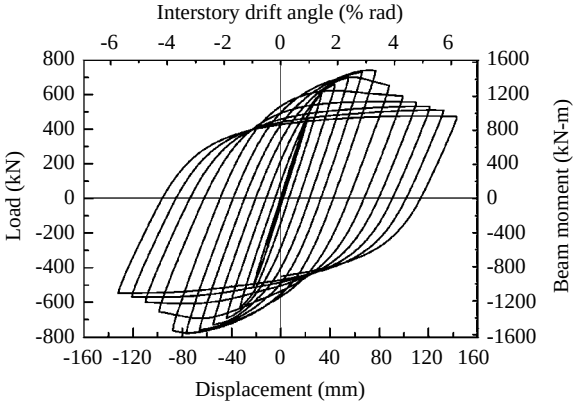

Fig. 7 Load-displacement relation (Hysteretic loops) of specimen SRC1-BOX-N

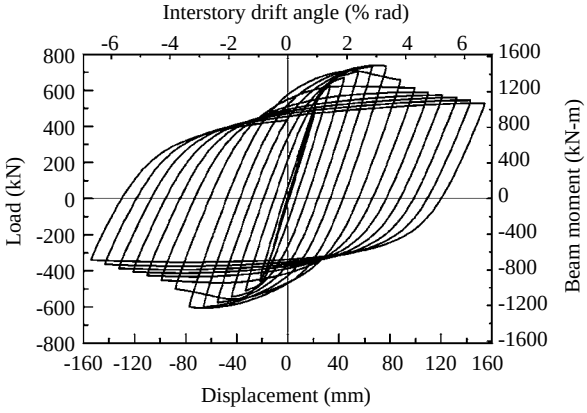

Fig. 8 Load-displacement relation (Hysteretic loops) of specimen SRC2-BOX-S

SRC2-BOX-S when the steel beam plastic rotation angles reached 3.1% and 6.0% radians, respectively.

Photos 7(a) and (b) were taken after the cyclic loading tests. With the successful formation of plastic hinges in both steel beams, it is also important to observe that, for both specimens SRC1-BOX-N and SRC2-BOX-S, the surfaces of the concrete in the connection zone were found to be able to remain in a sound condition without major cracks. This observation is interesting and will be further explained in section III.5.

2. Joint Rotation Analysis

Figure 9 shows a deflected beam-to-column joint (Cheng *et al*., 2000). The total displacement at beam tip, δ_t, is composed of two parts: the displacement due to the rotation of the SRC column, δ_{ct}, and the displacement resulting from the deflection of the steel beam, δ_{bt}. That is

$$\delta_t = \delta_{ct} + \delta_{bt} \tag{1}$$

The total angle of rotation of the joint, θ_t, corresponding to the beam tip total displacement is

$$\theta_t = \delta_t/(L_b + D/2) \tag{2}$$

where L_b is the distance from beam tip to column face;

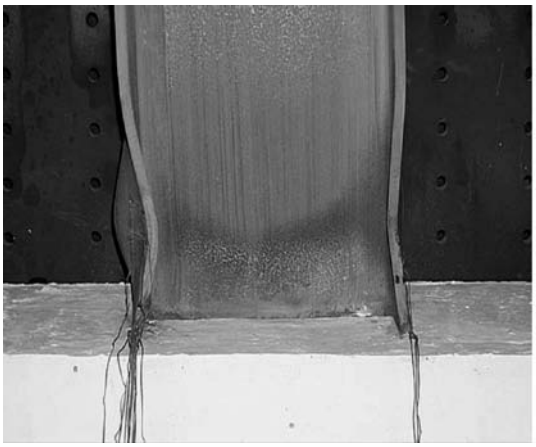

(a) Specimen SRC1–BOX–N: Steel beam tip displacement at $9\Delta_y$ (Beam plastic rotation θ_{bp} = 3.2% rad.)

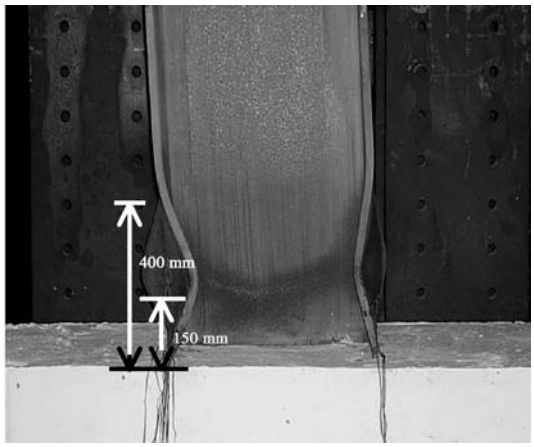

(b) Specimen SRC1–BOX–N: Steel beam tip displacement at 12 Δ_y (Beam plastic rotation θ_{bp} = 5.4% rad., Interstory drift angle $(\theta_t)_u$ = 6.2% rad.)

Photo 5 Steel beam plastic hinge of the specimen SRC1–BOX–N

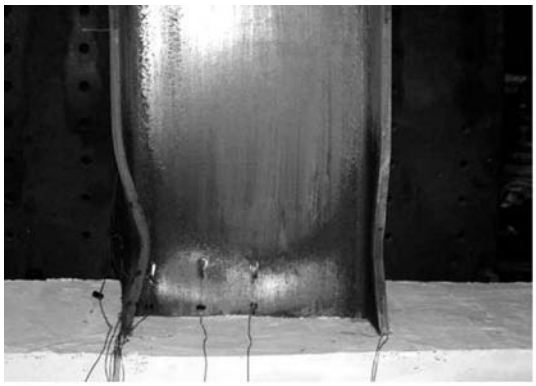

(a) Specimen SRC2–BOX–S: Steel beam tip displacement at $9\Delta_y$ (Beam plastic rotation θ_{bp} = 3.1% rad.)

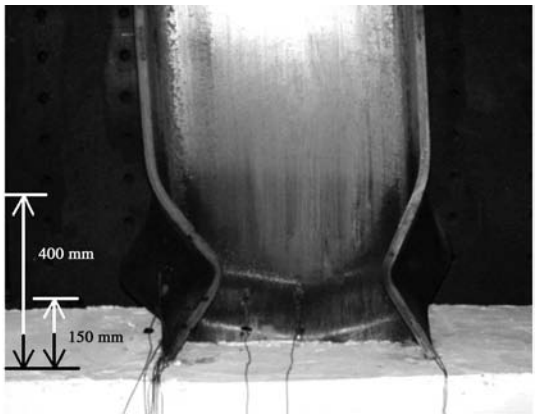

(b) Specimen SRC2–BOX–S: Steel beam tip displacement at 14 Δ_y (Beam plastic rotation θ_{bp} = 6.0% rad., Interstory drift angle $(\theta_t)_u$ = 6.7% rad.)

Photo 6 Steel beam plastic hinge of the specimen SRC2–BOX–S

(a) Specimen SRC1–BOX–N

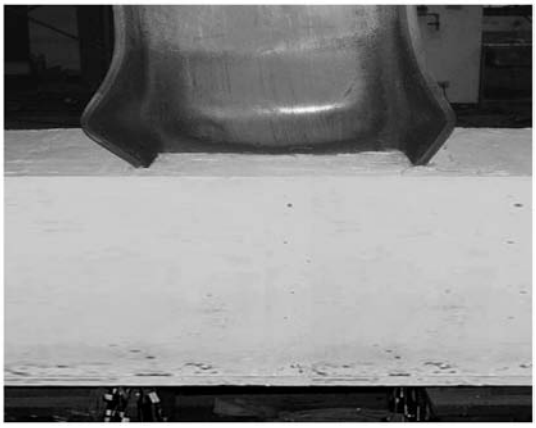

(b) Specimen SRC2–BOX–S

Photo 7 Final experimental results of specimens SRC1 and SRC2: (1) Steel beam developed satisfactory plastic hinge (2) Concrete remained sound at beam-to-column joint

Table 5 Rotation capacity of the steel beam-to-SRC column connections

Specimen designation	Loading direction	Total rotation of joint $(\theta_t)_u$ (rad)	SRC column rotation	Steel beam rotation		
			Total rotation θ_{ct} (rad)	Total rotation θ_{bt} (rad)	Elastic rotation θ_{be} (rad)	Plastic rotation θ_{bp} (rad)
		(1)	(2)	(3)	(4)	(5)
SRC1–BOX–N	+	6.20%	0.13%	6.07%	0.72%	5.35%
	–	5.72 %	0.11%	5.61%	0.84%	4.77%
SRC2–BOX–S	+	6.68 %	0.22%	6.46%	0.73%	5.73%
	–	6.68%	0.17%	6.51%	0.51%	6.00%

Note: (1) $(\theta_t)_u$ is the ultimate rotation angle of the connection when steel beam reached the maximum displacement; $(\theta_t)_u = (\delta_t)_u/(L_b + D/2)$
(2) θ_{ct} is the total rotation angle of the SRC column.
(3) θ_{bt} is the total rotation angle of the steel beam.
(4) θ_{be} is the elastic rotation angle of the steel beam.
(5) θ_{bp} is the plastic rotation angle of the steel beam.
(6) Correlations of angles: (1) = (2) + (3); (3) = (4) + (5); (5) = (1) – (2) – (4)

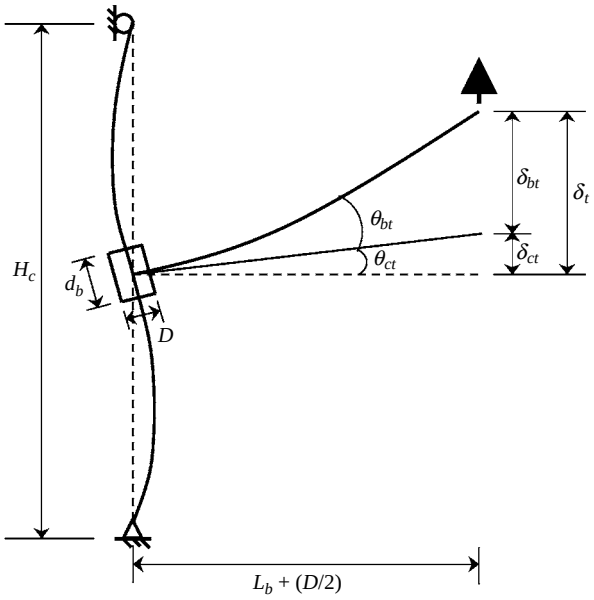

Fig. 9 Deflected shape of a beam-to-column joint (Cheng *et al.*, 2000)

D is the depth of the SRC column section. The beam tip total displacement δ_t was measured by recording the maximum horizontal travel distance of the MTS actuator at the beam tip.

The component of joint rotation due to the deflection of the SRC column, θ_{ct}, can be found from the displacements δ_1 and δ_2 measured by the two LVDTs placed at the joint, which gives

$$\theta_{ct} = (\delta_1 - \delta_2)/d_b \tag{3}$$

where d_b is the depth of the steel beam section. Thus the beam tip displacement caused by the rotation of the SRC column, δ_{ct}, is

$$\delta_{ct} = \theta_{ct}/(L_b + D/2) \tag{4}$$

Since the total displacement at beam tip, δ_t, was recorded with the MTS actuator, the beam tip displacement resulting from the deflection of the steel beam, δ_{bt}, is readily found as

$$\delta_{bt} = \delta_t - \delta_{ct} \tag{5}$$

Similarly, the component of joint rotation caused by the deflection of the steel beam, θ_{bt}, is

$$\theta_{bt} = \theta_t - \theta_{ct} \tag{6}$$

The inelastic rotation angle of the steel beam, θ_{bp}, is found by subtracting the elastic rotation angle of the steel beam, θ_{be}, from the total rotation angle of the steel beam, θ_{bt}, which gives

$$\theta_{bp} = \theta_{bt} - \theta_{be} \tag{7}$$

where $\theta_{bp} = M/k$, in which M is the beam moment; k is the elastic stiffness (i.e., the slope) determined from the linear part of the beam moment-rotation relation curve (M-θ curve). The k value was calculated as follows:

$$k = (M_2 - M_1)/(\theta_2 - \theta_1) \tag{8}$$

where M_2 and M_1 were taken as 20% and 60% of the yielding flexural strength M_y of the steel beam; θ_2 and θ_1 are the beam rotation angles corresponding to M_2 and M_1, respectively.

Based on the above analysis, Table 5 shows the

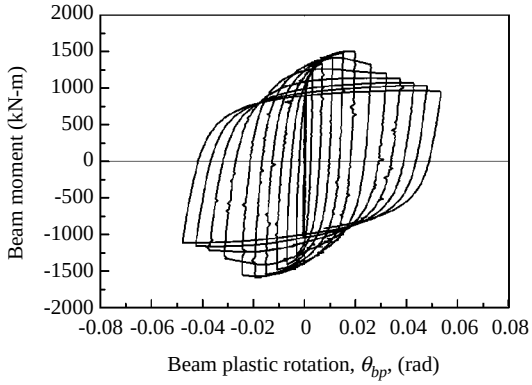

Fig. 10 Beam moment vs. Beam plastic rotation θ_{tp}: specimen SRC1–BOX–N

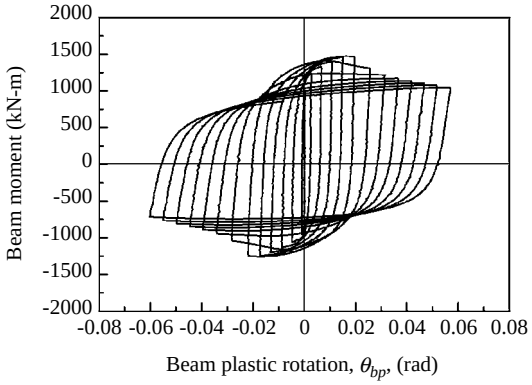

Fig. 11 Beam moment vs. Beam plastic rotation θ_{tp}: specimen SRC2–BOX–S

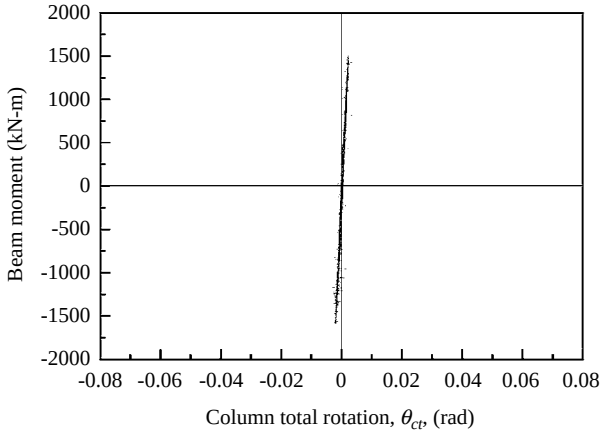

Fig. 12 Beam moment vs. SRC column rotation θ_{ct}: specimen SRC1–BOX–N

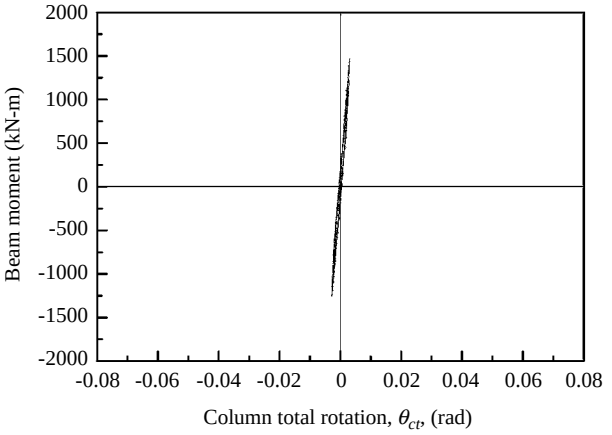

Fig. 13 Beam moment vs. SRC column rotation θ_{ct}: specimen SRC2–BOX–S

results of the beam-to-column joint rotation capacity of the two specimens tested in this study. The values shown in the table correspond to the rotation angles when the steel beam tip reached its maximum displacement. The angle $(\theta_t)_u$ represents the total rotation of the joint at the ultimate condition. The joint rotations caused by the deflection of SRC column, θ_{ct}, and by the deflection of steel beam, θ_{bt}, are also given in the table.

For specimen SRC1-BOX-N, it is observed from Table 5 that the total rotation of the beam-to-column joint at the ultimate condition, $(\theta_t)_u$, reached 6.20% and 5.72% radians in the positive and negative direction, respectively. The plastic rotation angle of the steel beam, θ_{bp}, reached 5.35% and 4.77% radians in the positive and negative direction, respectively. Similarly, for specimen SRC2-BOX-S, the total rotation of the joint at the ultimate condition, $(\theta_t)_u$, was 6.68% radians. The maximum plastic rotation angle of the steel beam, θ_{bp}, was 6.00% radians. It is obvious that both specimens demonstrated excellent ductility.

Figures 10 and 11 show the relations between the beam moment and the beam plastic rotation angle, θ_{bp}, for specimens SRC1-BOX-N and SRC2-BOX-S, respectively. In addition, Figs. 12 and 13 show the relations between the beam moment and the SRC column rotation, θ_{ct}. It is observed that the SRC column rotation angle is very small as compared to the steel beam plastic rotation angle. This means that most of the strain energy was consumed by the inelastic deformation of the steel beam. The very small rotation of the SRC column at the beam-to-column joint also explains how the surfaces of the concrete in the connection zone remained in a sound condition without major cracks.

3. Strain Variations at Beam-to-Column Joint

Figures 14 and 15 show the variations of the strain gage readings recorded from the steel beam flanges near the connection zone of specimens SRC1-BOX-N and SRC2-BOX-S, respectively. As shown in Fig.

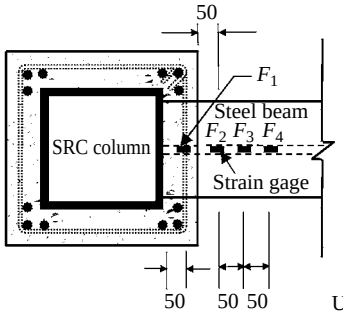

(a) Strain gage location on steel flange of specimen SRC1-BOX-N (strain gage F_1 is located within the joint and covered by concrete)

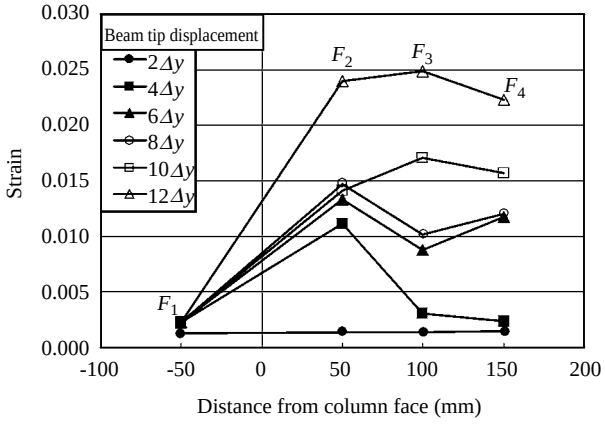

(b) Variations of strain gage readings on steel flange at different stages of beam tip displacement

Fig. 14 Strain gage readings on steel flange of specimen SRC1–BOX–N

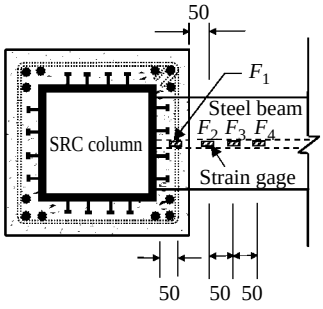

(a) Strain gage location on steel flange of specimen SRC2-BOX-N (strain gage F_1 is located within the joint and covered by concrete)

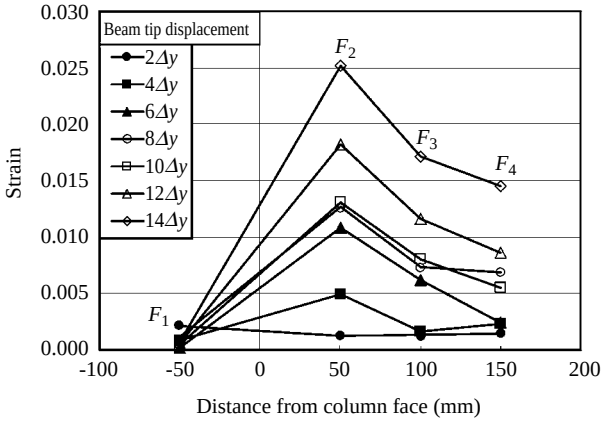

(b) Variations of strain gage readings on steel flange at different stages of beam tip displacement

Fig. 15 Strain gage readings on steel flange of specimen SRC2–BOX–S

14(b), it is interesting to observe that, at different stages of beam tip displacement, the readings of the strain gage F1 (located inside the connection zone and covered by concrete, as shown in Fig. 14(a)) were always at a relative low strain level throughout the entire cyclic loading history. A similar phenomenon is observed from Figs. 15(a) and (b) for specimen SRC2-BOX-S.

As in the observations mentioned in the previous section, the reinforced concrete in the connection zone may provide an "effective constraint" to the portion of steel beam embedded in the SRC column. The relatively low level of the strain reading of strain gage F1 seems to support this observation. Because the portion of steel beam embedded in the SRC column was confined by the reinforced concrete, the steel beam was not allowed to develop a large plastic deformation inside of the SRC column.

If we take a look of the stain readings from the strain gages located at 50, 100 and 150 mm away from the SRC column face, it is obvious that the recorded strain readings increased sharply when the beam tip displacement became larger than $4\Delta_y$. This observation suggests that the plastic deformation became apparent at this level and the majority of the inelastic strain energy was absorbed by the steel beam outside of the face of the column.

The largest strain reading recorded from specimen SRC1-BOX-N was about 2.5% when the beam tip displacement reached $12\Delta_y$. Similarly, the largest strain reading recorded from specimen SRC2-BOX-S was also about 2.5% when the beam tip displacement reached $14\Delta_y$. If we compare the locations of the plastic hinges shown in Photos 5 and 6, they match well with the strain readings recorded from the test.

4. Influence of Shear Studs

Based on the cyclic loading test results, both the beam-to-column connection specimens showed excellent plastic deformation capability, regardless of the application of shear studs on the steel surfaces in the connection zone.

For specimen SRC1-BOX-N in which no shear studs were applied, the connection was found to be able to sustain an interstory drift angle of 6.2%

Table 6 Summary of test results of the steel beam-to-SRC column connections

Specimen designation	Steel beam		SRC column	Important test results			
	Reduced beam section (RBS)	Stiffened flange-plate or rib	Shear studs on steel box	Plastic[(1)] rotation angle of steel beam θ_{bp} (rad)	Interstory[(2)] drift angle of joint $(\theta_t)_u$ (rad)	Plastic hinge of steel beam	Concrete integrity at B-to-C joint
SRC1–BOX–N	No	No	No	5.35%	6.20%	Excellent	Remained sound
SRC2–BOX–S	No	No	Yes	6.00%	6.68%	Excellent	Remained sound

Note: (1) θ_{bp} is the plastic rotation angle of the steel beam at maximum displacement
(2) $(\theta_t)_u$ is the ultimate rotation angle of the connection when steel beam reached maximum displacement.

radians, which was significantly larger than the required minimum rotation capacity of 4% radians specified in the latest AISC seismic provisions (2005).

For specimen SRC2-BOX-S in which shear studs were applied, the connection could sustain an interstory drift angle up to 6.7% radians, which is slightly larger than the angle of 6.2% radians of specimen SRC1-BOX-N. However, the difference is relatively minor and may have little practical significance.

5. Seismic Performance of the Connections

Table 6 summarizes the major findings of this experimental study. In general, these two beam-to-column connections showed excellent seismic resistance capability. In Section 9.2 of the AISC seismic provisions (2005), it states that beam-to-column connections used in the seismic load resisting system (SLRS) shall satisfy the following requirements: (1) The connection shall be capable of sustaining an interstory drift angle of at least 0.04 radians; (2) The measured flexural resistance of the connection, determined at the column face, shall be at least $0.8M_p$ of the connected beam at an interstory drift angle of at least 0.04 radians, where M_p is the nominal plastic flexural strength.

It is noted that the interstory drift angles of the specimens SRC1 and SRC2 tested in this study reached 6.2% and 6.7% radians, respectively, which satisfy the minimum requirement of 0.04 radians. In addition, the measured flexural resistances of the connections SRC1 and SRC2 at drift angle of 0.04 radians were 1280 and 1210 kN-m, respectively, which are both larger than $0.8M_p$ of the connected beam ($0.8M_p = 0.8 \times 1293 = 1034$ kN-m). Therefore, the above two requirements of AISC seismic provisions are satisfied.

Along with the development of the plastic hinge in the steel beam, the test results also revealed that the concrete in the connection zone remained sound throughout the cyclic loading history. As shown in Photos 7(a) and (b), there was no major crack observed on the concrete surface. This phenomenon is interesting and may be explained as follows:

As shown in Table 4, for both specimens, the nominal shear strength of the steel box section in SRC column, $(V_n)_s$, is found to be significantly larger than the maximum required shear strength of the joint, $(V_u)_j$. The ratios of $(V_n)_s/(V_u)_j$ are 1.69 and 1.78 for specimens SRC1-BOX-N and SRC2-BOX-S, respectively. This observation suggests that the shear strength of the "two webs" of steel box section alone is strong enough to resist the maximum shear force at the beam-to-column joint, which occurs when the steel beam reaches its plastic moment capacity. Therefore, at the connection zone, the shear force was mainly resisted by the steel box section in the SRC column. The concrete was kept virtually unharmed because it was only subjected to relatively minor shear deformation throughout the loading process.

Furthermore, with the concrete at the connection zone remaining nearly intact, it is thus possible for this part of the reinforced concrete to provide an "effective constraint" to the embedded portion of the steel beam in the SRC column. This constraint assisted the steel beam to develop plastic deformation outside of the face of SRC column. Consequently, the plastic hinge of the steel beam was successfully "forced away" from the groove-welded joint.

From the above discussions, it becomes clear that, for a steel beam-to-SRC column connection, the reinforced concrete at the connection zone played a role similar to a "stiffening element" to the steel beam. As a result, the groove-welded joint of the steel beam to the steel box section in SRC column was protected by the concrete and avoided possible brittle damage. The mechanism described above is similar to that of a "stiffened end plate connection" or a "stiffened

flange plate connection" in the Special Moment Frame (SMF) described in FEMA-350 (2000). Its primary purpose is to force the steel beam plastic hinge "away" from the immediate neighborhood of the groove-welded joint at the beam-to-column connection, so that the welded joint can be protected from premature failure.

In addition, it is also important to note that each of the steel beams used in this study was directly welded to the steel box in the SRC column. There was no reduction made to the flanges of the steel beam (i.e., it was not a "reduced beam section, RBS"), nor was a stiffened-rib or flange-plate added to the steel beam at the connection zone. Thus, with the savings of the manufacturing cost of steel beam flange-cutting or plate-stiffening, both the connection specimens tested in this study demonstrated satisfactory seismic resistance capability.

IV. SUMMARY AND CONCLUSIONS

Based on the experimental results, the following conclusions can be drawn within the scope of this study:

1. Both of the full-scale steel beam-to-SRC column connections tested in this study demonstrated excellent seismic resistance capability. The steel beams of the connections were found to be able to develop plastic rotations in excess of 5% radians. Satisfactory interstory drift angle up to 6% radians was observed from the tests. It is noted that the steel beam was directly welded to the steel box section in the SRC column. There was no reduction of the flanges of the steel beam (i.e., it was not a "reduced beam section, RBS"), nor was a stiffened-rib or flange-plate added to the steel beam at the connection zone.
2. The specimen with shear studs attached on steel surfaces, SRC2-BOX-S, sustained an interstory drift angle of 6.7% radians, which is slightly larger than the 6.2% radians of specimen SRC1-BOX-N in which no shear studs was applied.
3. With the plastic hinges successfully developed in the steel beams outside of the SRC column face, the test results also showed that the concrete at the connection zone was found to be able to remain in a sound condition without major cracks.
4. For the steel beam-to-SRC column connections tested in this study, the reinforced concrete in the connection zone played an important role similar to a "stiffening element" for the steel beam. The reinforced concrete was able to provide an "effective constraint" to the embedded portion of the steel beam in the SRC column. This constraint successfully assisted the steel beam to develop plastic hinge outside of the SRC column face. As a result, the groove-welded joint of the steel beam to the steel box section in the SRC column was protected by the reinforced concrete and avoided possible brittle damage.
5. The mechanism described above is similar to that of a "stiffened end plate connection" or a "stiffened flange plate connection" in the Special Moment Frame (SMF) recommended in FEMA-350. Its primary purpose is to force the steel beam plastic deformation away from the immediate neighborhood of the groove-welded joint at the beam-to-column connection. Therefore, the plastic hinge can be successfully developed in the steel beam, and the welded joint can be protected from premature failure.

REFERENCES

ACI, 2005, *Buildings Code Requirements for Structural Concrete and Commentary (ACI 318M-05)*, American Concrete Institute, Farmington Hills, MI, USA.

AIJ, 2001, *Standards for Structural Calculation of Steel Reinforced Concrete Structures*, Architectural Institute of Japan, Tokyo, Japan.

AISC, 2005, *Specification for Structural Steel Buildings, American Institute of Steel Construction*, Chicago, IL, USA.

AISC, 2005, *Seismic Provisions for Structural Steel Buildings, American Institute of Steel Construction*, Chicago, USA.

Alostaz, Y. M., and Schneider, S. P., 1996, "Connections to Concrete Filled Steel Tubes," *Proceedings of the 11th World Conference on Earthquake Engineering*, Acapulco, Mexico, Paper No. 748.

Alostaz, Y. M., and Schneider, S. P., 1996, "Analytical Behavior of Connections to Concrete- Filled Steel Tubes," *Journal of Constructional Steel Research*, Vol. 40, No. 2, pp. 95-127.

Azizinamini, A., and Prakash, B. A., 1993, "Tentative Design Guideline for a new Steel Beam Connection Detail to Composite Tube Columns," *Engineering Journal*, American Institute of Steel Construction, 3rd Quarter, pp. 108-115.

Cheng, C. T., Huang, P. H., Lu, L. Y., and Chung, L. L., 2000, "Connection Behaviors of Steel Beam to Concrete-Filled Circular Steel Tubes," *Report No. NCREE-00-009*, National Center for Research in Earthquake Engineering, Taipei, Taiwan.

Chiew, S. P., Lie, S. T., and Dai, C. W., 2001, "Moment Resistance of Steel I-Beam to CFT Column Connections," *Journal of Structural Engineering*, ASCE, Vol. 127, No. 10, pp. 1164-1172.

Chou, C. C., and Uang, C. M., 2002, "Cyclic Performance of a Type of Steel Beam to Steel-Encased Reinforced Concrete Column Moment Connection,"

Journal of Constructional Steel Research, Vol. 58, Issue 5-8, pp. 637-663.

ECCS, 1994, *Design of Composite Steel and Concrete Structures, Part 1.1: General Rules and Rules for Buildings*, ENV 1994-1-1: Eurocode 4, European Convention for Constructional Steelwork.

Elremaily, A., Azizinamini, A., and Filippou, F., 1997, "Development of Design Criteria for Steel Beam to CFT Column Connections in Seismic Regions," *U.S.-Japan Cooperative Earthquake Research Program: Composite and Hybrid Structures, 4th JTCC*.

FEMA, 2000, "Recommended Seismic Design Criteria for New Steel Moment Frame Buildings- FEMA-350," Prepared by SAC Joint Venture for Federal Emergency Management Agency, Washington, D.C., USA.

FEMA, 1994, "Recommended Provisions for the Development of Seismic Regulations for New Buildings- FEMA-222A," National Earthquake Hazards Reduction Program, Building Seismic Safety Council, Washington, D.C., USA.

Hsu, C. Y., 2003, "Effect of Panel Zone Shear Strength on Seismic Resistance of Steel Beam to SRC Column Connections," *Master Thesis*, Department of Civil Engineering, National Chiao Tung University, Hsinchu, Taiwan.

MIF, 2004, *Building Code for Design of Steel Reinforced Concrete (SRC) Structures*. Ministry of Interior Affairs, Taipei, Taiwan.

Nishiyama, I., Fujimoto, T., Fukumoto, T., and Yoshioka, K., 2004, "Inelastic Force-Deformation Response of Joint Shear Panels in Beam-Column Moment Connections to Concrete-Filled Tubes," *Journal of Structural Engineering*, ASCE, Vol. 130, No. 2, pp. 244-252.

Ricles, J. M., Peng, S. W., and Lu, L. W., 2004, "Seismic Behavior of Composite Concrete Filled Steel Tube Column-Wide Flange Beam Moment Connections," *Journal of Structural Engineering*, ASCE, Vol. 130, No. 2, pp. 223-232.

Ricles, J. M., Lu, L. W., Sooi, T. K., Vermaas, G. W., and Graham, W. W., 1996, "Experimental Performance of Moment Connections in CFT Column-WF Beam Structural Systems under Seismic Loading," *Proceedings of the 11th World Conference on Earthquake Engineering*, Acapulco, Mexico, Paper No. 1224.

Schneider, S. P., 1997, "Summary of Connections to Concrete-Filled Steel Tube Columns," *U.S.-Japan Cooperative Earthquake Research Program: Composite and Hybrid Structures, 4th JTCC*.

Wakabayashi, M. A., 1987, "Historical Study of Research on Composite Construction in Japan," *Proceedings of the Conference on Composite Construction in Steel and Concrete*, ASCE, NY, USA, pp. 400-427.

Yang, C. H., 2003, "Effect of Flexural Strength Ratio on Seismic Resistance of Steel Beam to SRC Column Connections," *Master Thesis*, Department of Civil Engineering, National Chiao Tung University, Hsinchu, Taiwan.

Manuscript Received: Apr. 10, 2007
Revision Received: Aug. 24, 2007
and Accepted: Sep. 04, 2007